SCIENTIFIC REPORTS

OPEN

Origin of giant piezoelectric effect in lead-free $K_{1-x}Na_xTa_{1-y}Nb_yO_3$ single crystals

Received: 25 January 2016
Accepted: 20 April 2016
Published: 10 May 2016

Hao Tian[1,*], Xiangda Meng[1,*], Chengpeng Hu[1], Peng Tan[1], Xilong Cao[1], Guang Shi[1], Zhongxiang Zhou[1] & Rui Zhang[2]

A series of high-quality, large-sized (maximum size of 16 × 16 × 32 mm³) $K_{1-x}Na_xTa_{1-y}Nb_yO_3$ ($x = 0.61$, 0.64, and 0.70 and corresponding $y = 0.58$, 0.60, and 0.63) single crystals were grown using the top-seed solution growth method. The segregation of the crystals, which allowed for precise control of the individual components of the crystals during growth, was investigated. The obtained crystals exhibited excellent properties without being annealed, including a low dielectric loss (0.006), a saturated hysteresis loop, a giant piezoelectric coefficient d_{33} ($d_{33} = 416$ pC/N, determined by the resonance method and $d_{33}^* = 480$ pC/N, measured using a piezo-d_{33} meter), and a large electromechanical coupling factor, k_{33} ($k_{33} = 83.6\%$), which was comparable to that of lead zirconate titanate. The reason the piezoelectric coefficient d_{33} of $K_{0.39}Na_{0.61}Ta_{0.42}Nb_{0.58}O_3$ was larger than those of the other two crystals grown was elucidated through first-principles calculations. The obtained results indicated that $K_{1-x}Na_xTa_{1-y}Nb_yO_3$ crystals can be used as a high-quality, lead-free piezoelectric material.

Piezoelectric materials are used widely in a variety of applications, including in ultrasonic transducers and piezoelectric transformers and sensor. For the last 60 years, lead zirconate titanate (PZT) ceramics were the most popular piezoelectric materials, owing to their excellent piezoelectric properties[1–3]. However, because lead causes significant harm to the environment and human health, efforts have been made to develop lead-free piezoelectric materials[4,5]. It is widely believed that potassium sodium niobate ($K_{1-x}Na_xNbO_3$, KNN)-based materials have great potential as replacements for lead-based piezoelectric materials because of their excellent properties and because their Curie temperatures (T_C) are higher than those of other lead-free materials such as barium titanate (BT) and bismuth sodium titanate (BNT)[6–8].

In 2004, Y. Saito *et al.* reported the large piezoelectric effect in Li, Ta, Sb co-doped KNN ceramics. A major breakthrough was the fact that the piezoelectric coefficient d_{33} of these KNN-based ceramics was as high as 416 pC/N[6]. Since then, intensive research efforts have been made to improve the piezoelectric properties of KNN-based ceramics[9–16]. As is known, the properties of single crystals are better than those of ceramics of the same composition. Furthermore, in order to investigate the mechanism responsible for the large piezoelectric effect observed in doped KNN and to improve the performance of KNN-based materials, it is important to grow KNN-based single crystals. Recently, several methods for growing KNN-based crystals have been reported, and each method has its advantages and disadvantages. The most widely used methods for growing KNN-based single crystals are the flux, Bridgman, and top-seed solution growth (TSSG) methods. The flux method yields crystals of good quality; however, the as-grown crystals are difficult to study, owing to their small size[17–19]. Chen *et al.* successfully grew Li:KNN single crystals with a large d_{33} (405 pC/N) using the Bridgman method; however, the single crystals contained oxygen vacancies and defects, which led to a high leakage current, as was evident from their polarization vs. electric field hysteresis loops[20]. Zheng *et al.* grew Li, Ta, Sb-doped KNN single crystals using the TSSG method and investigated their piezoelectric properties. They were able to obtain $K_{0.561}Na_{0.439}Nb_{0.768}Ta_{0.232}O_3$ ($d_{33} = 200$ pC/N, $k_{33} = 82.7\%$), $(K_{0.487}Na_{0.513}Li_{0.01\sim0.04})(Nb_{0.667}Ta_{0.333})O_3$ ($d_{33} = 354$ pC/N, $k_{33} = 81.5\%$), and $(K_{0.51}Na_{0.49}Li_{0.02\sim0.03})(Nb_{0.67}Ta_{0.32}Sb_{0.01})O_3$ ($d_{33} = 172$ pC/N, $k_{33} = 52.3\%$)[21–23]. For the lack of continuous changes in the composition and doping ions, the research of the contribution of doping ions on the piezoelectric

[1]Department of Physics, Harbin Institute of Technology, Harbin 150001, China. [2]Condensed Matter Science and Technology Institute, Harbin Institute of Technology, Harbin 150001, China. *These authors contributed equally to this work. Correspondence and requests for materials should be addressed to H.T. (email: tianhao@hit.edu.cn) or Z.Z. (email: 23326579@qq.com)

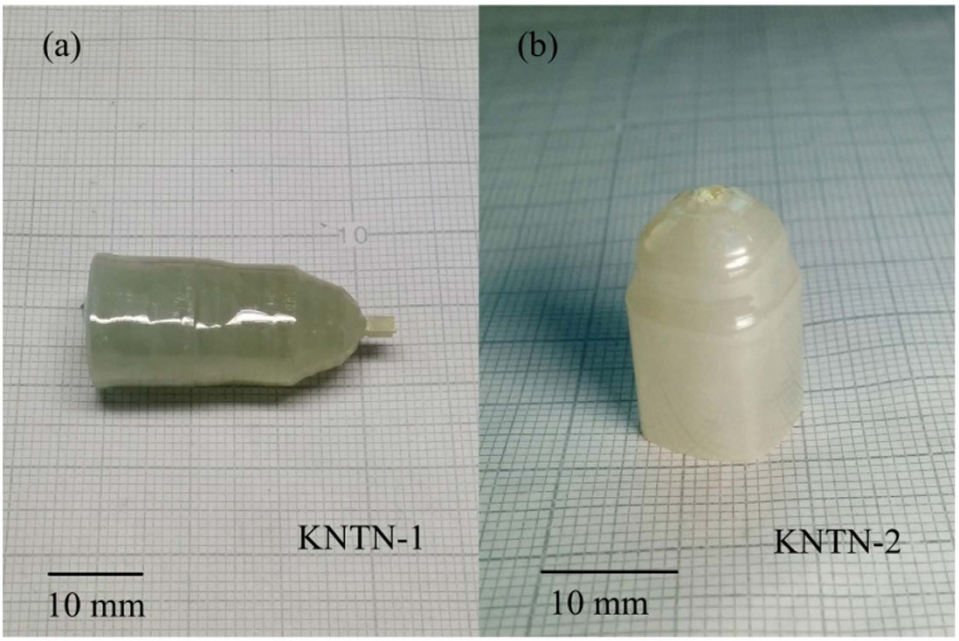

Figure 1. Photographs of the as-grown KNTN single crystals.

Composition of the KNTN crystal	K/Na in the melt		Ta/Nb in the melt	
$K_{0.30}Na_{0.70}Ta_{0.37}Nb_{0.63}O_3$	75:25		10:90	
$K_{0.36}Na_{0.64}Ta_{0.40}Nb_{0.60}O_3$	75:25		15:85	
$K_{0.39}Na_{0.61}Ta_{0.42}Nb_{0.58}O_3$	75:25		18:82	
Segregation of K	Segregation of Na	Segregation of Ta	Segregation of Nb	T_g(°C)
0.400	2.800	3.700	0.700	1193.0
0.480	2.560	2.667	0.706	1245.0
0.520	2.440	2.333	0.707	1277.5

Table 1. Segregation of potassium, sodium, tantalum, and niobium and the growth temperatures of $K_{1-x}Na_xTa_{1-y}Nb_yO_3$crystals.

properties of KNN is difficult. Furthermore, there have been few microscopic studies on the physical mechanism responsible for the improvement in the piezoelectric properties after doping with Ta.

In this paper, we report the successful growth of a series of high-quality, large-sized $K_{1-x}Na_xTa_{1-y}Nb_yO_3$ (KNTN) single crystals using the TSSG method. The segregation of the crystals, which allowed for precise control over the individual components of the crystals, was investigated. The as-grown crystals exhibited excellent properties, including a saturated hysteresis loop, a giant piezoelectric coefficient, d_{33}^* (480 pC/N), and a large electromechanical coupling factor, k_{33} (83.6%); the values of these parameters were comparable to those of PZT. Finally, the origin of the high piezoelectric effect observed in the crystals was elucidated through first-principles calculations.

Results and Discussion

Photographs of the as-grown KNTN crystals are shown in Fig. 1. The dimensions of the largest KNTN crystal grown were $16 \times 16 \times 32\,mm^3$, which are much greater than those of previously reported KNTN crystals. The crystals were transparent at temperatures higher than their Curie temperature (T_C), and no cracks were observed in them. At room temperature, the crystals were milky white, because of the presence of polydomains, which scatter light. The KNTN crystals were shaped like a square with round corners, and the surfaces of the crystals were $(100)_C$ and $(010)_C$ faces.

The segregation of the crystals allowed for precise control of the individual components of the crystals during the growth process. The relationships between the composition of the KNTN crystals; the ratio of the potassium and sodium concentrations in the melt; the ratio of the tantalum and niobium concentrations in the melt; the segregation coefficient of potassium, sodium, tantalum, and niobium; and the growth temperature (T_g) are shown in Table 1. The segregation coefficient of potassium (S^K) was calculated from the equation: $S^K = C_c^K/C_m^K$, where C_c^K is K concentration in single crystal; C_m^K is K concentration in melt. The similar calculations were performed for the S^{Na}, S^{Ta}, S^{Nb}. The segregation of ion was determined by their properties. Moreover, it was also determined by ion concentration in melt and the condition of growth. With an increase in the tantalum content in the melt, the

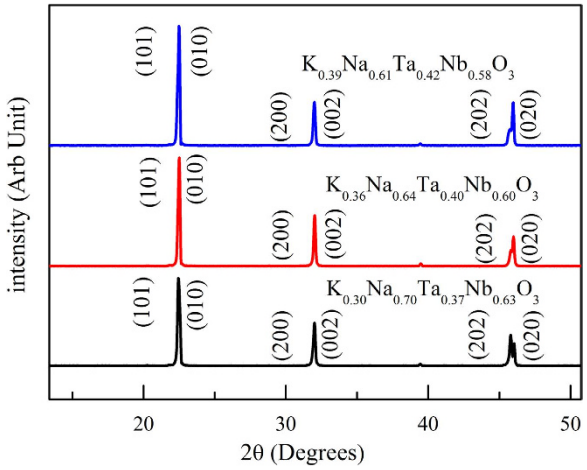

Figure 2. X-ray powder diffraction patterns of the as-grown $K_{1-x}Na_xTa_{1-y}Nb_yO_3$ crystals.

Crystal	*a*(Å)	*b*(Å)	*c*(Å)
$K_{0.30}Na_{0.70}Ta_{0.37}Nb_{0.63}O_3$	5.6061	3.9385	5.5876
$K_{0.36}Na_{0.64}Ta_{0.40}Nb_{0.60}O_3$	5.6083	3.9433	5.5828
$K_{0.39}Na_{0.61}Ta_{0.42}Nb_{0.58}O_3$	5.6290	3.9449	5.5828
$K_{0.3}Na_{0.7}NbO_3$[40]	5.64304	3.93187	5.61260

Table 2. Lattice parameters of the KNTN crystals. [a]The lattice parameters corresponding to a symmetric orthorhombic cell were converted into the lattice parameters for a pseudo-monoclinic cell ($a' = c'$, b, and β) using the following formula $a = 2d \sin(\beta/2)$, $c = 2a' \sin(\beta/2)$[41].

growth temperature increased from 1193 °C to 1277.5 °C. On the other hand, the segregation coefficient of tantalum decreased from 3.700 to 2.333, which in accordance with the phase diagram of the $KTaO_3$-$KNbO_3$ system[24]. Further, the segregation coefficient of potassium increased from 0.400 to 0.520, while that of sodium decreased from 2.800 to 2.560. This was in contradiction to the phase diagram of the $KNbO_3$-$NaNbO_3$ system[25] and meant that the doping of Ta into the KNN system affected the segregation of K and Na.

The XRD patterns indicated that the crystals had pure perovskite-like structures and did not contain any secondary phases (Fig. 2). The as-grown KNTN single crystals were in the orthorhombic phase at room temperature. From the XRD data, the lattice parameters of the KNTN crystals were determined using the software Jade 6.0; the results are shown in Table 2. The (202) and (020) peaks moved to the high degrees decreases in x and y, resulting in increases in the lattice parameters "a" and "b." These changes in the lattice parameters of the KNTN crystals indicated that the volume of the lattice cell increased with the decrease in x and y. The cation radius of the tantalum $r(Ta^{5+})$ is slightly smaller than that of the niobium $r(Nb^{5+})$, while the volume of the as-grown crystals increase with decrease of Nb concentration (as Table 2 shown). Thus the main reason for the increase in the volume was the fact that the cation radius of potassium $r(K^+)$ is larger than that of sodium $r(Na^+)$.

The temperature dependence of the dielectric constant of the $K_{1-x}Na_xTa_{1-y}Nb_yO_3$ crystals at 1 kHz is shown in Fig. 3. The two peaks in the curves represent the orthorhombic-tetragonal phase-transition temperature ($T_{O\text{-}T}$) and the Curie temperature (T_C), respectively; the values of these temperatures were consistent with the XRD results and suggested that the crystals were in the orthorhombic phase at room temperature. As can be seen from the data listed in Table 3, with the tantalum and sodium content varying, the value of $T_{O\text{-}T}$ of the KNTN crystals decreased from 84 °C to 39 °C. Concomitantly, the value of T_C decreased from 228 °C to 161 °C. According to the data of pure KNN single crystals[26], we can determine that the value of $T_{O\text{-}T}$ and T_C of the KNN crystals slightly increased with decrease of Na concentration. However, the T_C of KTN single crystals gotten by the function $T_C = 676x + 32$ K (x is the Nb concentration in KTN crystals)[27] decreased with doping Ta. Thus, the variation of $T_{O\text{-}T}$ and T_C mainly owed to Ta/Nb ratio[28]. In addition, the dielectric property (ε_r) of the as-grown KNTN crystals increased with the increase in the potassium and tantalum contents, and is larger than that of the pure KNN single crystals. The result is mainly reasonable because Ta could move the $T_{O\text{-}T}$ peak left, and room temperature is close to the $T_{O\text{-}T}$ peak. The quality of $K_{0.39}Na_{0.61}Ta_{0.42}Nb_{0.58}O_3$ was better than the other two components crystals as its tanδ was the smallest. Furthermore, it was similar or smaller than that of the crystals reported previously in the literature[26,29].

Figure 4a showed the *P-E* hysteresis loops of the KNTN crystals at 25 °C at a frequency of 200 Hz under a maximum electric field of 35 kV/cm. All as-grown crystals exhibit saturated curves at an electric field of 35 kV/mm, which suggests that as-grown crystals were of high quality. The values of the coercive field (E_c), remanent polarization (P_r), and spontaneous polarization (P_s) of the KNTN single crystals as well as those of the pure KNN single crystals are listed in Table 4. The E_c, P_r, and P_s values of the KNTN crystals were smaller than those of pure KNN single crystals. The result is in good agreement with the difference between Ta^{5+} and Nb^{5+} in unit

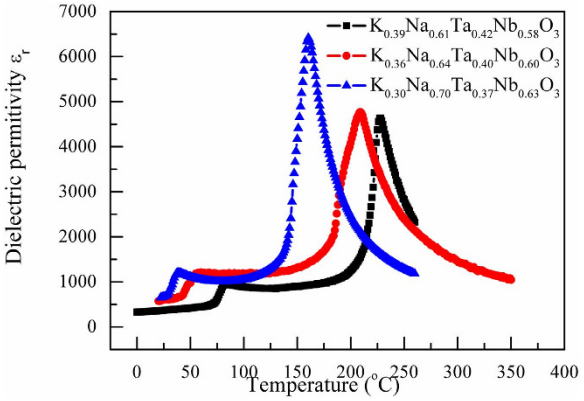

Figure 3. Temperature dependence of the dielectric constant of the $K_{1-x}Na_xTa_{1-y}Nb_yO_3$ crystals at 1 kHz.

Crystal	$T_{O\text{-}T}$ (°C)	T_C (°C)	ε_r at T_{room}	tanδ at T_{room} (%)
$K_{0.30}Na_{0.70}Ta_{0.37}Nb_{0.63}O_3$	84	228	369	0.7
$K_{0.36}Na_{0.64}Ta_{0.40}Nb_{0.60}O_3$	58	209	609	0.7
$K_{0.39}Na_{0.61}Ta_{0.42}Nb_{0.58}O_3$	39	161	670	0.6
$K_{0.334}Na_{0.666}NbO_3$[26]	174	395	68	0.4
$K_{0.5}Na_{0.5}NbO_3$ [1$\bar{3}$1][29]	192	410	1015	1

Table 3. The $T_{O\text{-}T}$, T_C, dielectric constant (ε_r), and dielectric loss (tanδ) values of the KNTN single crystal at a frequency of 1 kHz.

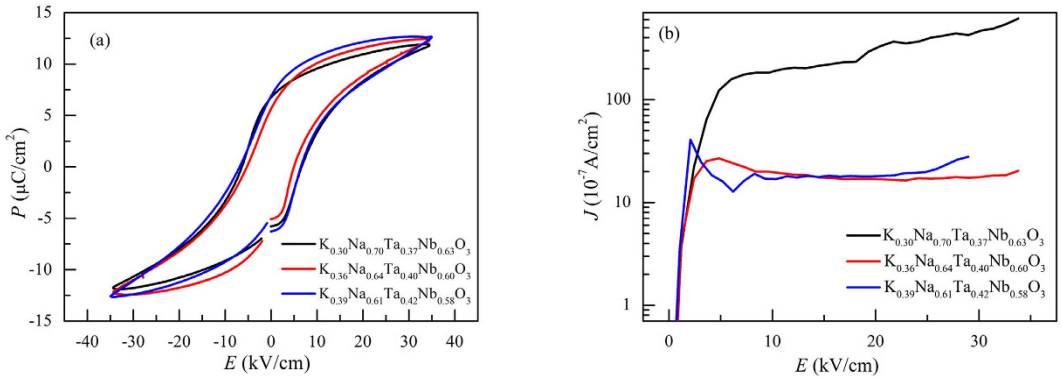

Figure 4. (**a**) *P-E* hysteresis loops of the KNTN crystals at room temperature at a frequency of 200 Hz. (**b**) Values of the leakage current density (*J*) at room temperature along the $[001]_C$ direction of the KNTN crystals.

	E_c (kV/cm)	P_r (μC/cm^2)	P_s (μC/cm^2)
$K_{0.30}Na_{0.70}Ta_{0.37}Nb_{0.63}O_3$	6.52	6.11	9.14
$K_{0.36}Na_{0.64}Ta_{0.40}Nb_{0.60}O_3$	5.05	5.37	10.34
$K_{0.39}Na_{0.61}Ta_{0.42}Nb_{0.58}O_3$	6.73	6.59	9.86
$K_{0.334}Na_{0.666}NbO_3$[26]	11.59	~12	~12
$K_{0.455}Na_{0.545}NbO_3$[26]	11.11	~12	~12

Table 4. Coercive field (E_c), remanent polarization (P_r), and spontaneous polarization (P_s) values of the $K_{1-x}Na_xTa_{1-y}Nb_yO_3$ single crystals.

cell. Ta^{5+} and Nb^{5+} ions were randomly distributed in the B-sites. Because Nb^{5+} ions moving along the 12 directions of spontaneous polarization mainly contribute to the P_r, the P_r decreased with doping Ta. The values of the room-temperature leakage current density (*J*) along the $[001]_C$ direction of the as-grown KNTN crystals are

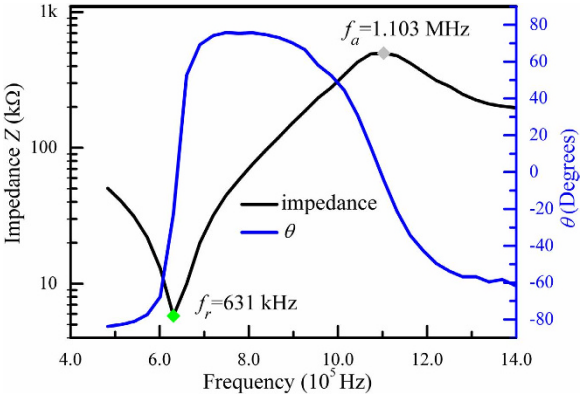

Figure 5. Room-temperature k_{33} resonator impedance spectra of $K_{0.39}Na_{0.61}Ta_{0.42}Nb_{0.58}O_3$ single crystal.

shown in Fig. 4b. The leakage currents for the KNTN crystals which were not annealed at high temperature had an order of magnitude of ~10^{-5} A/cm^2, which is far lower than that for KNN crystals grown by the flux method (10^{-3} to 10^{-4} A/cm^2)[30,31]. This result suggested that there were less O^{2-} vacancies in the crystals grown by TSSG method[26], which was another indication of the high quality of the KNTN single crystals grown in this study. Because of the more O^{2-} vacancies of $K_{0.30}Na_{0.70}Ta_{0.37}Nb_{0.63}O_3$ caused by the lower melting temperature, the J of that was one order of magnitude larger than other two single crystals.

The piezoelectric vibrators were cut along the $[001]_c$ direction, and their impedance spectra (magnitude of impedance $|Z|$ and phase angle, θ, vs. frequency) were measured, so that their piezoelectric parameters could be calculated. A typical longitudinal extension response for the k_{33} resonator of $K_{0.39}Na_{0.61}Ta_{0.42}Nb_{0.58}O_3$ single crystal was shown in Fig. 5. For this k_{33} resonator, a resonance frequency (f_r) was 631 kHz while an antiresonance frequency (f_a) was 1.103 MHz. The values of the elastic compliance constant s_{33}, electromechancical coupling factor k_{33}, and piezoelectric coefficient d_{33} of the samples were calculated by substituting the measured long-size l, f_r and f_a into the following equation: $k_{33}^2 = (\pi f_r/(2f_a))\tan[\pi(f_a - f_r)/(2f_a)]$, $s_{33}^D = 1/[\rho(2lf_a)^2]$, $s_{33}^E = s_{33}^D/(1 - k_{33}^2)$, $d_{33} = k_{33} \cdot \sqrt{\varepsilon_{33}^T \cdot s_{33}^E}$. The maximum phase angle was approximately 75°; this was indicative of the existence of a polydomain state (domain engineered). The similar measurement was performed for other k_{33}, k_{31}, and k_t resonators. The k_{33} values of the samples were between 76.4% and 83.6% and larger than those reported previously for KNN-TL and PZT5A. Further, the giant piezoelectric coefficient d_{33} of the $K_{0.39}Na_{0.61}Ta_{0.42}Nb_{0.58}O_3$ crystal was 416 pC/N, as determined by the resonance method, while d_{33}^* was 480 pC/N, as measured with a piezo-d_{33} meter; these values are larger than those for other two as-grown single crystals and KNN-TL. As can be seen from the data, the values of most of the parameters of $K_{0.39}Na_{0.61}Ta_{0.42}Nb_{0.58}O_3$ which were greatly influenced by temperature were comparable to those of PZT5A.

As shown in Table 5, the piezoelectric coefficient d_{33} of the $K_{0.39}Na_{0.61}Ta_{0.42}Nb_{0.58}O_3$ crystal was larger than those of the $K_{0.30}Na_{0.70}Ta_{0.37}Nb_{0.63}O_3$ and $K_{0.36}Na_{0.64}Ta_{0.40}Nb_{0.60}O_3$ crystals. This can be attributed to the polymorphic phase transition (PPT) which was lowered to room temperature by Ta, when the K/Na ratio was far away from 0.5/0.5[32,33]. However, the microscopic physical mechanism responsible was not involved. To elucidate the origin of the high piezoelectric effect in the microcosmic, we used first-principles calculations to calculate the free energy of the lattice cell.

Spontaneous polarization occurs in twelve directions along $[011]_C$ in the orthorhombic ($mm2$)-phase single crystals, while it occurs in six directions along $[001]_C$ for the tetragonal ($4mm$) -phase single crystals (shown in Fig. 6). When an electric field was applied along the z-axis, the directions in which spontaneous polarization occurred in the orthorhombic phase changed to those corresponding to the tetragonal phase. In addition, according to a previous study, the reason the piezoelectric coefficient d_{33} of the grown crystals was large was that the polarization directions were rotated and not stretched[34]. The internal energies of the $K_{1-x}Na_xTa_{1-y}Nb_yO_3$ crystals corresponding to the different phases (orthorhombic phase, U_o, and tetragonal phase, U_t) were calculated through first-principles calculations. For this, we calculated the internal energies of potassium tantalate ($KTaO_3$, KT), potassium niobate ($KNbO_3$, KN), sodium tantalate ($NaTaO_3$, NT), and sodium niobate ($NaNbO_3$, NN), as well as the weighted averages[35,36] of the individual coefficients. The obtained results are shown in Table 6.

It can be seen that ΔU decreased from 3.0241 eV/Å^3 to 2.5666 eV/Å^3 with an increase in the Ta fraction from 0.37 to 0.42 and an increase in the K fraction from 0.30 to 0.39. Further, the difference in the free energies of the orthorhombic and tetragonal phases of $K_{0.39}Na_{0.61}Ta_{0.42}Nb_{0.58}O_3$ in the absence of an electric field was the lowest. Thus, when an electric field was applied, the domain of $K_{0.39}Na_{0.61}Ta_{0.42}Nb_{0.58}O_3$ which was at PPT temperature, was the easiest to rotate, which can enhance piezoelectric properties[34]. The conclusion was the same as that calculated by Landau – Devonshire model in $BaTiO_3$ – based materials[37,38] and PZT-based materials[39]. As a result, its piezoelectric coefficient was larger than those of $K_{0.30}Na_{0.70}Ta_{0.37}Nb_{0.63}O_3$ and $K_{0.36}Na_{0.64}Ta_{0.40}Nb_{0.60}O_3$.

Conclusions

In this study, a series of large-sized (size of largest crystal = 16 × 16 × 32 mm^3) orthorhombic $K_{1-x}Na_xTa_{1-y}Nb_yO_3$ (x = 0.61, 0.64, and 0.70 and corresponding y = 0.58, 0.60, and 0.63) single crystals were grown using the TSSG method. The crystals exhibited excellent dielectric, piezoelectric, and ferroelectric properties, including

Piezoelectric materials	Elastic compliance constants s^E, s^D(10^{-12} m^2/N)					
	s_{11}^E		s_{33}^E		s_{11}^D	s_{33}^D
$K_{0.30}Na_{0.70}Ta_{0.37}Nb_{0.63}O_3$	10.9		14.8		9.17	6.14
$K_{0.36}Na_{0.64}Ta_{0.40}Nb_{0.60}O_3$	12.7		19.2		9.98	6.60
$K_{0.39}Na_{0.61}Ta_{0.42}Nb_{0.58}O_3$	14.5		26.6		11.01	8.01
KNN-TL[22]	17.2		27.0		13.4	9.08
PZT5A[42]	16.4		18.8		14.4	9.46
	Electromechanical coupling factors k			Piezoelectric coefficient d (10^{-12}C/N)		
	k_t	k_{31}	k_{33}	d_{31}	d_{33}	d_{33}^{*} [a]
$K_{0.30}Na_{0.70}Ta_{0.37}Nb_{0.63}O_3$	65.9%	39.5%	76.4%	−87.6	197	220
$K_{0.36}Na_{0.64}Ta_{0.40}Nb_{0.60}O_3$	63.0%	46.0%	81.0%	−147	319	360
$K_{0.39}Na_{0.61}Ta_{0.42}Nb_{0.58}O_3$	62.6%	49.2%	83.6%	−181	416	480
KNN-TL[22]	45.1%	47%	81.5%	−163	354	–
PZT5A[42]	49%	34%	70.5%	−171	374	–
	Dielectric constants ε_r and β ($10^{-3}/\varepsilon_0$)					
	ε_{33}^T		ε_{33}^S		β_{33}^T	β_{33}^S
$K_{0.30}Na_{0.70}Ta_{0.37}Nb_{0.63}O_3$	510		168		1.96	5.97
$K_{0.36}Na_{0.64}Ta_{0.40}Nb_{0.60}O_3$	915		275		1.09	3.63
$K_{0.39}Na_{0.61}Ta_{0.42}Nb_{0.58}O_3$	1055		334		0.95	2.99
KNN-TL[22]	790		234		1.27	4.28
PZT5A[42]	1700		830		0.59	1.20

Table 5. Piezoelectric parameters of the as-grown KNTN single crystals poled along $[001]_c$ and having tetragonal 4*mm* symmetry. [a]Measured using a piezo-d_{33} meter.

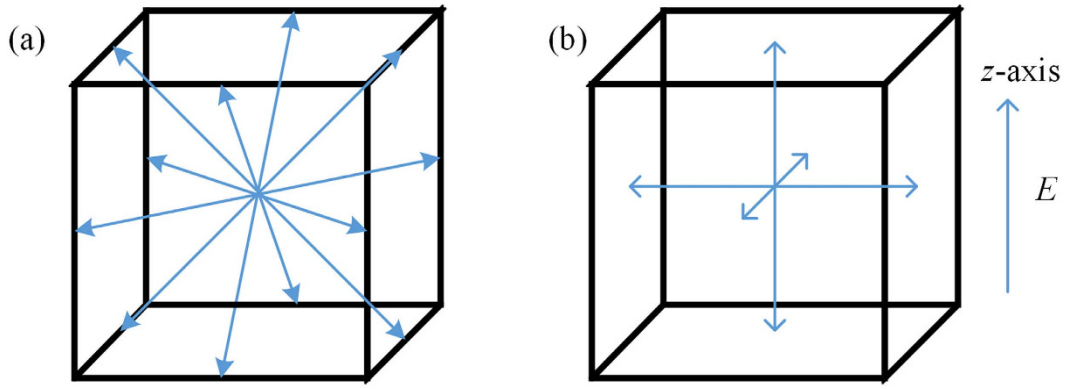

Figure 6. Directions of spontaneous polarization of the KNTN crystals in the orthorhombic and tetragonal phases: (**a**) spontaneous polarization directions of the orthorhombic phase and (**b**) spontaneous polarization directions of the tetragonal phase.

$K_{1-x}Na_xTa_{1-y}Nb_yO_3$	U_o(eV/Å^3)	U_t (eV/Å^3)	$\Delta U = U_t - U_o$ (eV/Å^3)
$K_{0.30}Na_{0.70}Ta_{0.37}Nb_{0.63}O_3$	50.7596	53.7836	3.0241
$K_{0.36}Na_{0.64}Ta_{0.40}Nb_{0.60}O_3$	49.6940	52.4140	2.7200
$K_{0.39}Na_{0.61}Ta_{0.42}Nb_{0.58}O_3$	49.0279	51.5945	2.5666

Table 6. Internal energies of the $K_{1-x}Na_xTa_{1-y}Nb_yO_3$ crystals.

a giant d_{33}^{*} (480 pC/N) and a large k_{33} (83.6%). The leakage currents of the $K_{1-x}Na_xTa_{1-y}Nb_yO_3$ crystals were very low and of the order of 10^{-5} A/cm^2. The piezoelectric properties of the $K_{1-x}Na_xTa_{1-y}Nb_yO_3$ crystals improved with an increase in the potassium and tantalum contents when the phase of the $K_{1-x}Na_xTa_{1-y}Nb_yO_3$ crystals was orthorhombic. Finally, the difference in the free energies of the orthorhombic and tetragonal phases of $K_{0.39}Na_{0.61}Ta_{0.42}Nb_{0.58}O_3$ in the absence of an electric field was 2.5666 eV/Å^3; this was determined by first-principles calculations. This crystal was the smallest of the grown single crystals. Further, its domain was the easiest to rotate. Therefore, it exhibited the best piezoelectric properties.

Methods

As mentioned above, the KNTN single crystals were grown by the TSSG method. The raw materials used were powders of K_2CO_3 (99.99%), Na_2CO_3 (99.99%), Ta_2O_5 (99.99%), and Nb_2O_5 (99.99%). They were weighted to obtain a composition of $K_{1-x}Na_xTa_{1-y}Nb_yO_3$, with 10 mol% excess of K_2CO_3 and Na_2CO_3 (($K_2CO_3 + Na_2CO_3$): ($Ta_2O_5 + Nb_2O_5$) = 1.1:1) as the self-flux. The raw materials were mixed with ethanol, ball-milled for 24 h, and subsequently dried in an oven at 85 °C to volatilize the ethanol. Then, the mixture was calcined at 950 °C for 6 h to synthesize a KNTN polycrystal. The polycrystal was melted in a medium-frequency induction furnace at 1250 °C ~ 1375 °C, which is ~100 °C higher than the temperature for crystal growth, in order to eliminate the residual carbon dioxide and mix the compounds at the atomic level. Then, the temperature was decreased to the growth temperature, and a single crystal began to grow on a $[001]_C$ seed that was cut from a high-quality potassium tantalate niobate crystal. During crystal growth, the rotational and pulling rates were 15 r/min and 0.25 mm/h, respectively. After the completion of the growth process, the as-grown crystal was cooled to the room temperature at 35 °C/h.

The compositions of the as-grown crystals were determined by electron microprobe analysis (EPMA-1720, Shimadzu, Kyoto, Japan). The structures of the crystals were confirmed by X-ray diffraction (XRD) analyses (XRD-6000, Shimadzu, Kyoto, Japan). The crystals were oriented using a Laue X-ray machine. The $(001)_C$ in pseudo cubic structure structure surfaces of the samples were covered with silver electrodes, and the dielectric properties of the samples were measured as functions of the temperature using an inductance – capacitance – resistance (LCR) meter (E4980A, Agilent Technologies, Santa Rosa, CA). The polarization vs. electric field (*P-E*) hysteresis loops of the crystals were measured at 200 Hz using the ferroelectric test system (Precision Premier II, Radiant Technology, Inc., Albuquerque, NM, USA); the leakage current densities of the crystals were recorded using the same instrument. Cuts of the crystals with dimensions similar to those mentioned in IEEE standards were poled in silicon oil at a temperature of $T_{O\text{-}T} - 10$ °C under an electric field of 30 kV/cm. The resonance and antiresonance frequencies were measured using an HP 4294 A impedance phase analyzer. The piezoelectric coefficients and electromechanical coupling factors were determined at the resonance and antiresonance frequencies, according to the IEEE standards. The piezoelectric constant d_{33}^* was measured using a piezo-d_{33} meter (Zj-3A, Institute of Acoustics, Academic Sinica, Beijing, China).

References

1. Liu, Y. *et al.* Long, X. A new (1−x)Pb(Lu1/2Nb1/2)O_3−x$PbTiO_3$ binary ferroelectric crystal system with high Curie temperature. *Cryst Eng Comm.* **15,** 1643–1650 (2013)
2. He, C. *et al.* Compositional dependence of properties of Pb(Yb1/2Nb1/2)O_3-Pb(Mg1/3Nb2/3)O_3-$PbTiO_3$ ternary ferroelectric crystals. *Cryst Eng Comm.* **14,** 4513–4519 (2012).
3. Zhang, Q.-M., Wang, H., Kim, N. & Cross, L.-E. Direct evaluation of domainwall and intrinsic contributions to the dielectric and pie-zoelectric response and their temperature dependence on lead zir-conatetitanate ceramics. *J. Appl. Phys.* **75,** 454–459 (1994).
4. Wang, K. *et al.* Temperature-Insensitive (K, Na)NbO_3 -Based Lead-Free Piezoactuator Ceramics. *Adv. Funct. Mater.* **23,** 4079 (2013).
5. Hollenstein, E., Davis, M., Damjanovic, D. & Setter, N. Piezoelec-tric properties of Li- and Ta-modified (K0.5Na0.5)NbO_3 ceramics. *Appl. Phys. Lett.* **87,** 182905 (2005).
6. Saito, Y. *et al.* Lead-free piezoceramics. *Nature.* **432,** 84–87 (2004).
7. Zhang, S., Xia, R. & Shrout, T.-R., Lead-free piezoelectric ceramics vs. PZT? *J. Eelectroceram.* **19,** 251–257 (2007).
8. Shrout, T.-R. & Zhang, S.-J. Lead-free piezoelectric ceramics: Alternatives for PZT? *J. Electroceram.* **19,** 111–124 (2007).
9. Guo, Y., Kakimoto, K. & Ohsato, H. Phase transitional behavior and piezoelectric properties of Na0.5K0.5NbO_3-$LiNbO_3$ ceramics. *Appl. Phys. Lett.* **85,** 4121–4123 (2004).
10. Du, H., Zhou, W., Zhu, D. & Fa, L. Sintering Characteristic, Microstructure, and Dielectric Relaxor Behavior of (K0.5Na0.5) NbO3–(Bi0.5Na0.5)TiO_3 Lead-Free Ceramics. *J. Am. Ceram. Soc.* **91(9),** 2903–2909 (2008).
11. Zhang, B. *et al.* Lead-free Piezoelectrics Based on Potassium−Sodium Niobate with Giant d_{33}. *ACS Appl. Mater. Inter*. **5,** 7718–7725 (2013).
12. Wang, X. *et al.* New Potassium−Sodium Niobate Ceramics with a Giant d_{33}. *ACS Appl. Mater. Inter*. **6,** 6177–6180 (2014).
13. Wang, X. *et al.* Giant Piezoelectricity in Potassium−Sodium Niobate Lead-Free Ceramics. *J. Am. Chem. Soc.* **136,** 2905–2910 (2014).
14. Wang, X. *et al.* Large d_{33} in (K, Na)(Nb,Ta,Sb)O_3-(Bi, Na, K)ZrO_3 lead-free ceramics. *J. Mater. Chem. A*. **2,** 4122–4126 (2014).
15. Cheng, X., Li, Z. & Wu, J. Colossal permittivity in ceramics of TiO_2 Co-doped with niobium and trivalent cation. *J. Mater. Chem. A*. **3,** 5805–5810 (2015).
16. Zheng, T. & Wu, W. Enhanced piezoelectricity over a wide sintering temperature (400–1050 °C) range in potassium sodium niobate-based ceramics by two step sintering. *J. Mater. Chem. A*. **3,** 6772–6780 (2015).
17. Fisher, J.-G., Bencan, A. & Kosec, M. Growth of Dense Single Crystals of Potassium Sodium Niobate by a Combination of Solid-State Crystal Growth and Hot Pressing. *J. Am. Ceram. Soc.* **91,** 1503–1507 (2008).
18. Bencan, A., Tchernychova, E., Godec, M., Fisher, J. & Kosec, M. Compositional and Structural Study of a (K0.5Na0.5)NbO_3 Single Crystal Prepared by Solid State Crystal Growth. *Microsc. Microanal.* **15,** 435–440 (2009).
19. Farooq, M.-U. & Fisher, J.-G. Growth of (K0.5Na0.5)NbO_3-$SrTiO_3$ lead-free piezoelectric single crystals by the solid state crystal growth method and their characterization. *Ceram. Int.* **40,** 3199–3207 (2014).
20. Chen, K., Xu, G., Yang, D., Wang, X. & Li, J. Dielectric and pie-zoelectric properties of lead-free 0.95(K0.5Na0.5) NbO_3–0.05 $LiNbO_3$ crystals grown by the Bridgman method. *J. Appl. Phys.* **101,** 044103 (2007).
21. Zheng, L. *et al.* Large size lead-free (Na, K)(Nb, Ta)O_3 piezoelectric single crystal: growth and full tensor properties. *Cryst Eng Comm.* **15,** 7718 (2013).
22. Huo, X. *et al.* High quality lead-free (Li, Ta) modi-fied (K, Na)NbO_3 single crystal and its complete set of elastic, die-lectric and piezoelectric coefficients with macroscopic 4mm sym-metry. *CrystEngComm.* **16(42),** 9828–9833 (2014).
23. Wang, J. *et al.* Growth and characteri-zation of lead-free ferroelectric (K, Na, Li)(Nb, Ta, Sb)O_3 single crystal. *J. Cryst. Growth.* **409,** 39–43 (2015).
24. Reisman, A., Triebwasser, S. & Holtzberg, F. Phase Diagram of the System $KNbO_3$-$KTaO_3$ by the Methods of Differential Thermal and Resistance Analysis. *J. Am. Chem. Soc.* **77(16),** 4228–4230 (1955).
25. Ringgaard, E. & Wurlitzer, T. Lead-free piezoceramics based on alkali niobates. *J. Eur. Ceram. Soc.* **25(12),** 2701–2706 (2005).
26. Tian, H. *et al.* Top-Seeded Solution Growth and Properties of K1−xNaxNbO_3 Crystals. *Crystal Growth & Design.* **15(3),** 1180–1185 (2015).
27. Matthias, B. T. & Remeika, J. P. Dielectric properties of sodium and potassium niobates. *Physical Peview*. **82,** 727 (1951).
28. Wu, J., Xiao, D. & Zhu, J. Potassium−Sodium Niobate Lead-Free Piezoelectric Materials: Past, Present, and Future of Phase Boundaries. *Chemical reviews.* **115(7),** 2559–2595 (2015).

29. Urši, H., Benan, A., Škarabot, M., Godec, M. & Kosec, M. Dielec-tric, ferroelectric, piezoelectric, and electrostrictive properties of K0.5Na0.5NbO_3 single crystals. *J. Appl. Phys.* **107,** 033705 (2010).
30. Kizaki, Y., Noguchi, Y. & Miyayama, M. Defect control for low leakage current in K0.5Na0.5NbO_3 single crystals. *Appl. Phys. Lett.* **89,** 142910 (2006).
31. Noguchi, Y. & Miyayama, M. Effect of Mn doping on the leakage current and polarization properties in K0.14Na0.86NbO_3 ferroelectric single crystals. *J. Ceram. Soc. Jap*. **118,** 711–716 (2010).
32. Skidmore, T. A., Comyn, T. P. & Milne, S. J. Temperature stability of ($[Na_{0.5}K_{0.5}NbO_3]_{0.93}$-$[LiTaO_3]_{0.07}$) lead-free piezoelectric ceramics. *Applied Physics Letters*. **94,** 222902 (2009).
33. Dai, Y., Zhang, X. & Zhou, G. Phase transitional behavior in $K_{0.5}Na_{0.5}NbO_3$–$LiTaO_3$ ceramics. *Applied physics letters*, **90,** 262903 (2007).
34. Fu, H. & Cohen, R.-E. Polarization rotation mechanism for ultra-high electromechanical response in single-crystal piezoelectrics. *Nature.* **403,** 281–283 (2000).
35. Tian, Hao. *et al.* Effects of Growth Temperature on Crystal Morphology and Size Uniformity in $KTa_{1-x}Nb_xO_3$ and $K_{1-y}Na_yNbO_3$ Single Crystals. *Crystal Growth & Design.* **16(1),** 325–330 (2015).
36. Gumennik, A., Kurzweil-Segev, Y. & Agranat, A. J. Electrooptical effects in glass forming liquids of dipolar nano-clusters embedded in a paraelectric environment. *Optical Materials Express*. **1(3),** 332–343 (2011).
37. Yao, Y. *et al.* Large piezoelectricity and dielectric permittivity in $BaTiO_3$-x$BaSnO_3$ system: The role of phase coexisting. *EPL*. **98(2),** 27008 (2012).
38. Zhou, C. *et al.* Triple-point-type morphotropic phase boundary based large piezoelectric Pb-free material—Ba (Ti0.8Hf0.2)O3-(Ba0.7Ca0.3)TiO_3. *Applied Physics Letters.* **100(22),** 222910 (2012).
39. Damjanovic, D. A morphotropic phase boundary system based on polarization rotation and polarization extension. *Applied Physics Letters.* **97(6),** 062906 (2010).
40. Baker, D.-W., Thomas, P.-A., Zhang, N. & Glazer, A.-M. Structural study of KxNa1−xNbO_3 (KNN) for compositions in the range x = 0.24–0.36. *ActaCryst. B*. **65,** 22–28 (2009).
41. Shirane, G., Newnham, R. & Pepinsky, R. Dielectric Properties and Phase Transitions of $NaNbO_3$ and (Na, K)NbO_3. *Phys. Rev.* **96,** 581 (1954).
42. Jaffe, H. & Berlincourt, D.-A. Piezoelectric Transducer Materials. *PROCEEDINGS OF THE IEEE.* **53(10),** 1372–1386 (1965).

Acknowledgements

This work was sugpported by the National Natural Science Foundation of China (Grant Nos 50902034 and 11074059), the Science Fund for Distinguished Young Scholars of Heilongjiang Province (Grant No. JC200710), and the Program for Innovation Research of Science at the Harbin Institute of Technology (No. B201504). The authors wish to thank the personnel at the Laboratory of Micro-Optics and Photonic Technology of Heilongjiang Province for assistance with the experiments.

Author Contributions

H.T. and Z.Z. generated the idea. H.T. and X.M. wrote the manuscript text. X.M. and C.H. designed the experimental schemes and grew the crystals. X.M. determined the piezoelectric and dielectric properties. P.T. determined the free energies by first-principles calculations. X.C. and G.S. confirmed the XRD spectrum. R.Z. measured the polarization vs. electric field (*P-E*) hysteresis loops. All authors discussed the results and substantially contributed to the manuscript.

Additional Information

Competing financial interests: The authors declare no competing financial interests.

How to cite this article: Tian, H. *et al.* Origin of giant piezoelectric effect in lead-free $K_{1-x}Na_xTa_{1-y}Nb_yO_3$ single crystals. *Sci. Rep.* **6**, 25637; doi: 10.1038/srep25637 (2016).